Figure for the aim4np Report

This file contains the figures to which reference is made in the text submitted to SESAM. There is one page per figure. At the beginning of the document, there is the front-page with all the logos from each partner, followed by a list of all figures, the figure captions and the page where the figures can be found in this document. Then the figures follow in the same order as they have to be introduced into the main text, such that the cross-reference are correct. If there are several sub-figures (a,b,c,d...) these sub-figures could be spread over several pages. In that case, the page indicated in the table refers to the page where the caption is written.

Automated in-line Metrology for Nanoscale Production

aim4np

Final Report

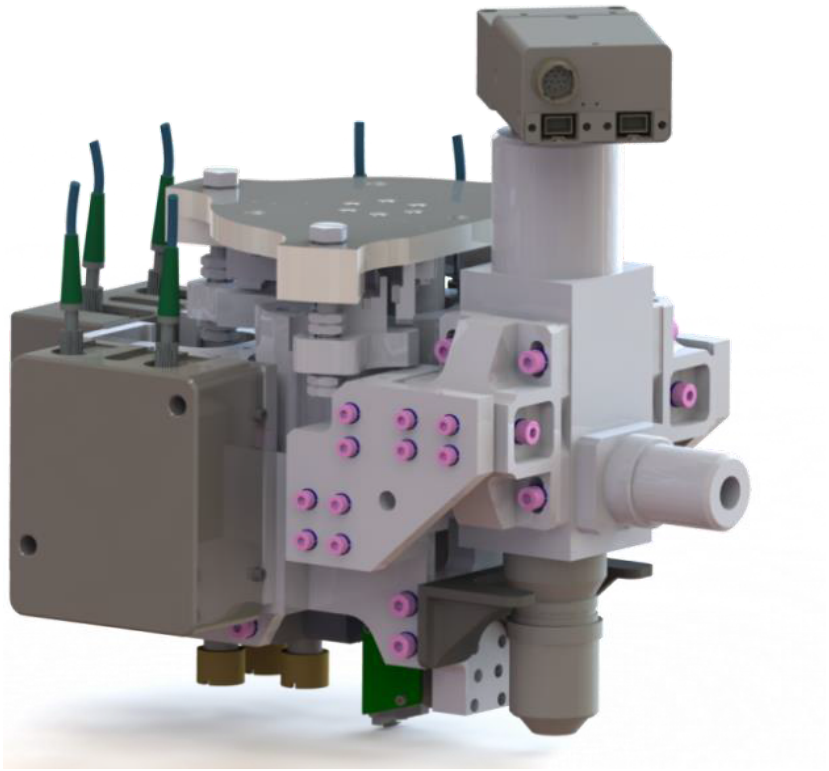

TU Delft

TU WIEN ACIN Automation & Control Institute Institut für Automatisierungs- & Regelungstechnik

CSIC CIN2 CNM

VSL Dutch Metrology Institute

NTC Weiz

nanosurf

SIOS Meßtechnik GmbH

NANO WORLD Innovative Technologies

Flubetech

nanotools scanning probes

IQS Persona Ciencia Empresa Universitat Ramon Llull

SEVENTH FRAMEWORK PROGRAMME

Figure Captions

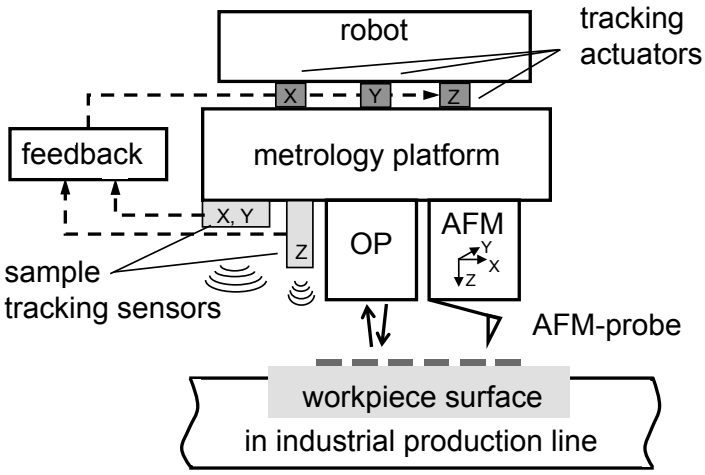

Figure 1 Concept of artificially locking the instrument suite to a work piece or part of a machine tool in a fabrication line, where the sample surface may vibrate. OP stands for a 3D optical probe e.g. a white-light interferometer for large area access.

a)

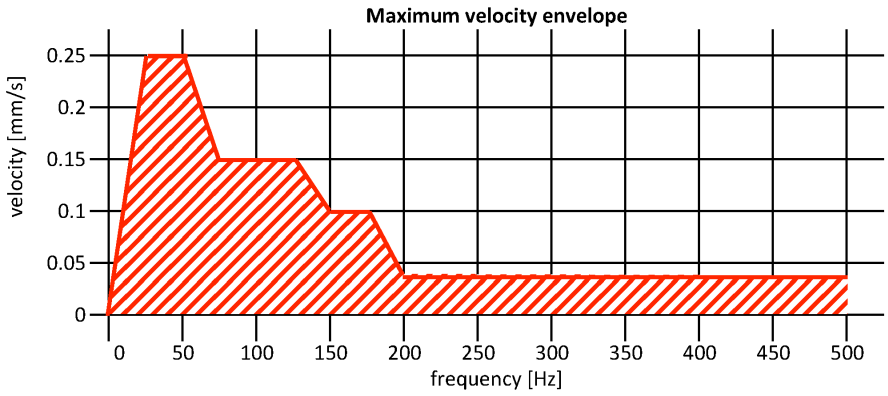

b)

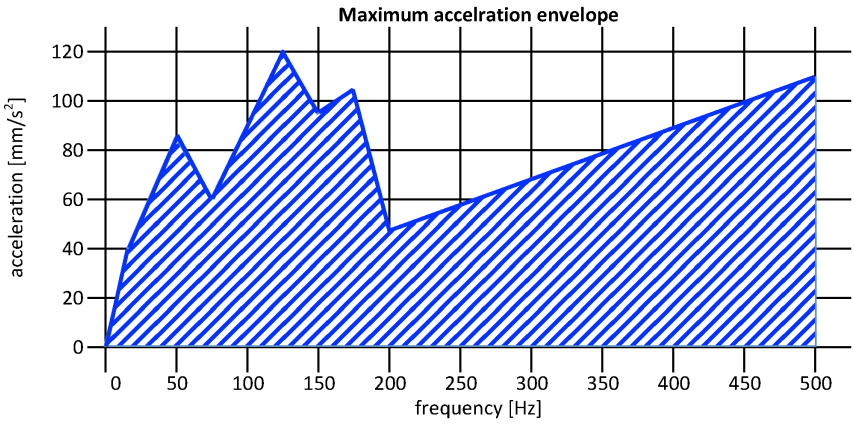

Figure 2 a) Maximum velocity envelope and
b) maximum acceleration envelope derived from experimental values

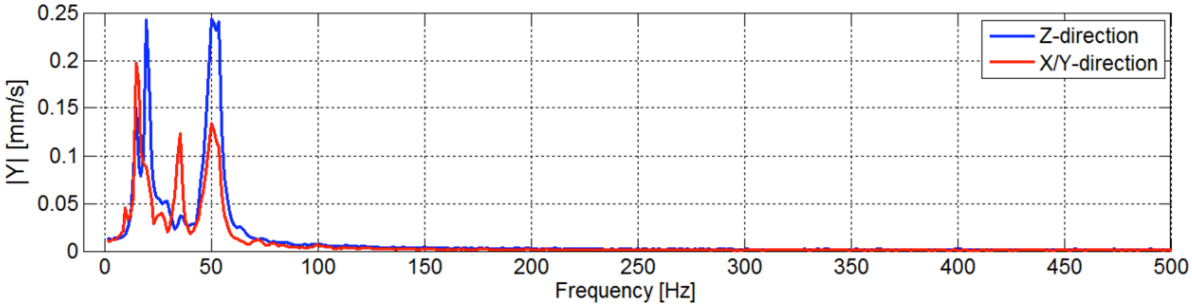

Figure 3 Measured and analysed worst-case velocity spectra of the robot with Waterfall-FFT timeslots of 0.8 seconds and a total measurement interval of 20 seconds.

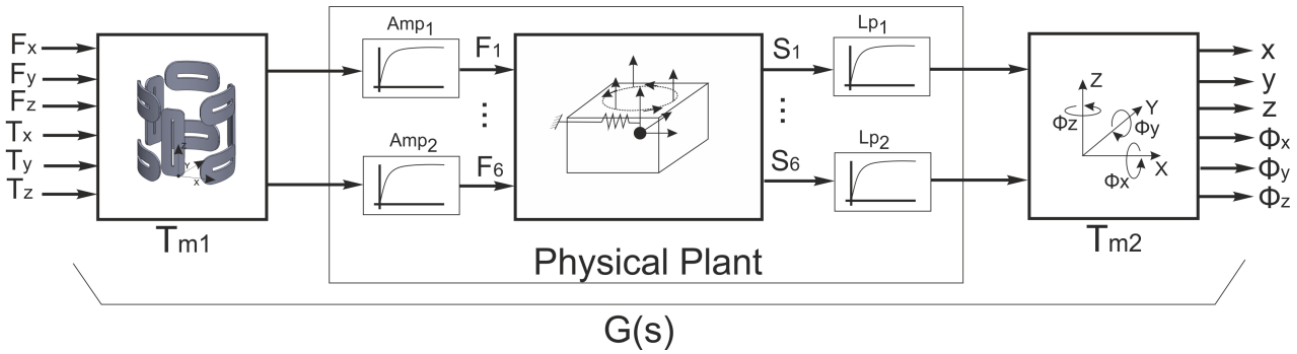

Figure 4 Schematics of the control loop with plant inputs (F1 ... F6) and plant output (S1 ... S6)

a)

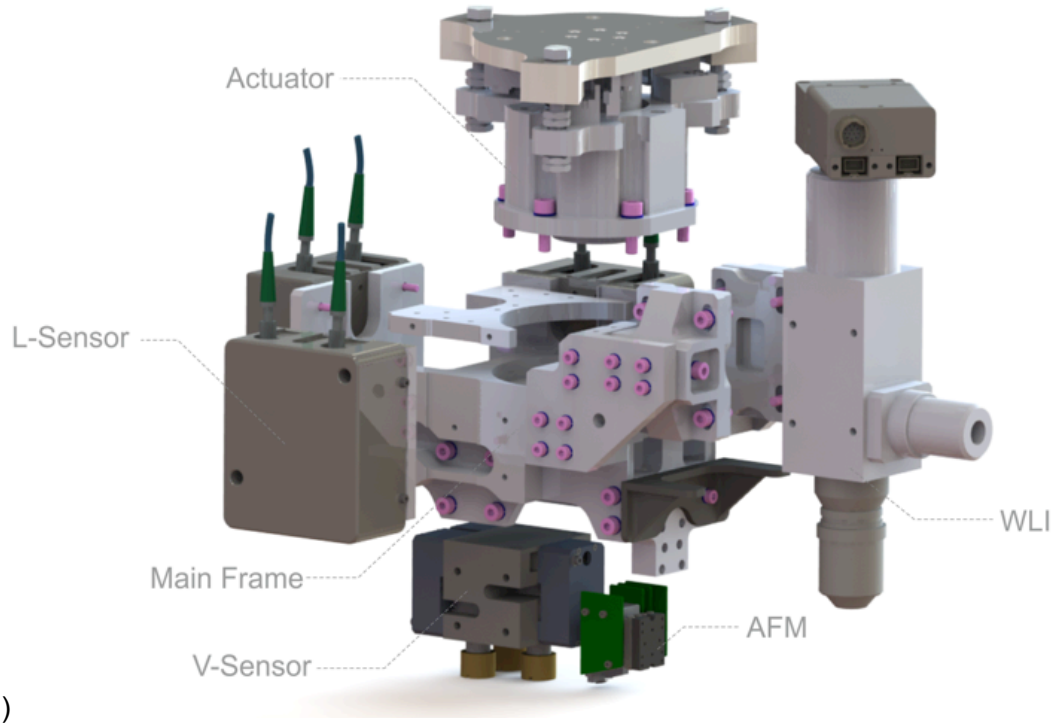

b)

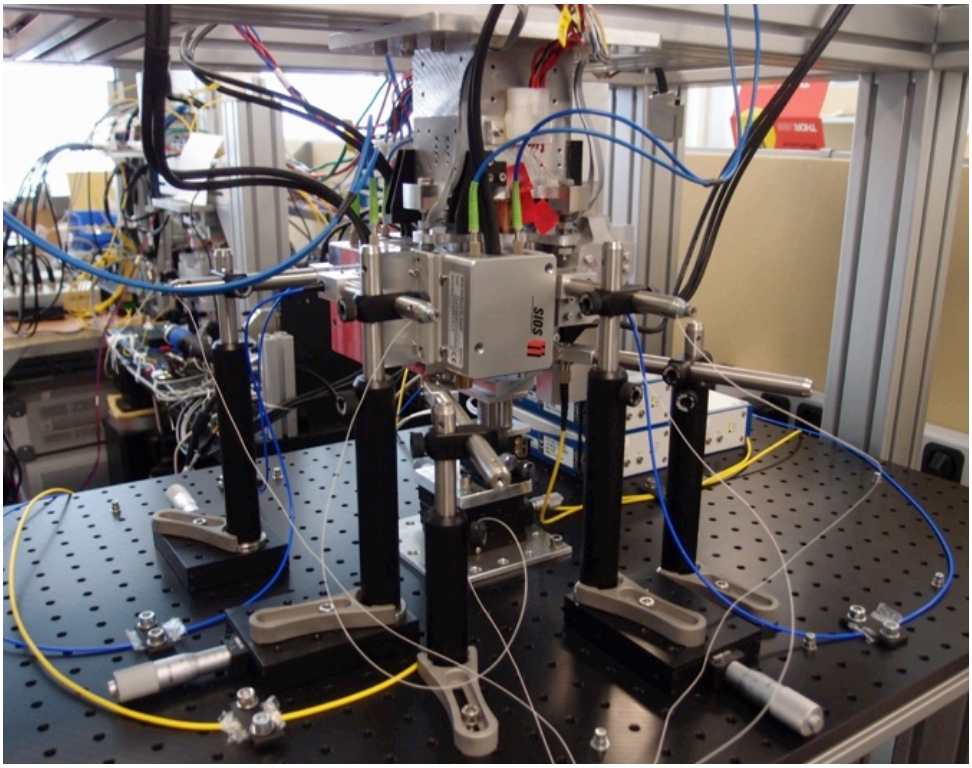

Figure 5 a) Explosion drawing of the CAD of the Metrology Platform and the different elements to be assembled to it.
b) The Metrology Platform in the test stage. The view is partially obstructed by cables and external tracking sensors that were added for test purposes.

a) 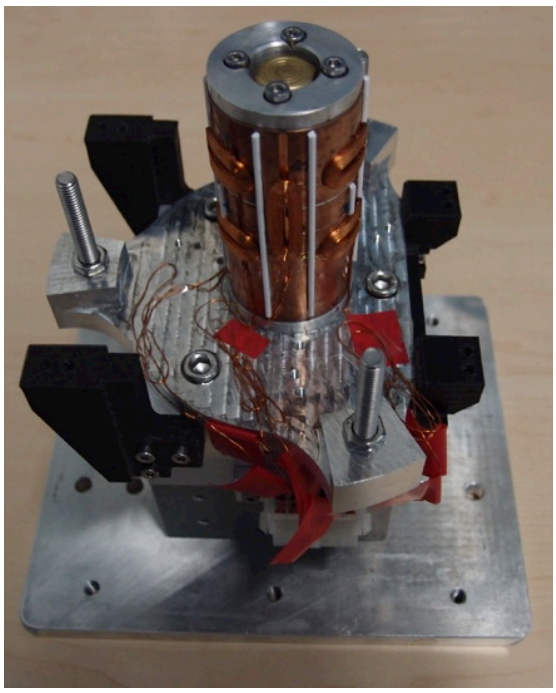

b) 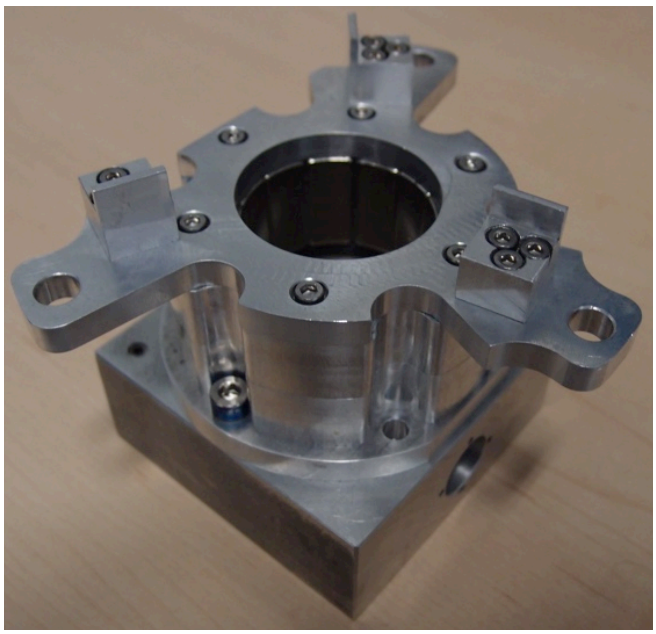

Figure 6: Tracking actuator fabricated by TU Vienna. The design is based on 3D-CAD drawings, which were delivered by TU Delft.
(a) Stator (up-side down) and
(b) mover of the actuator.

a)

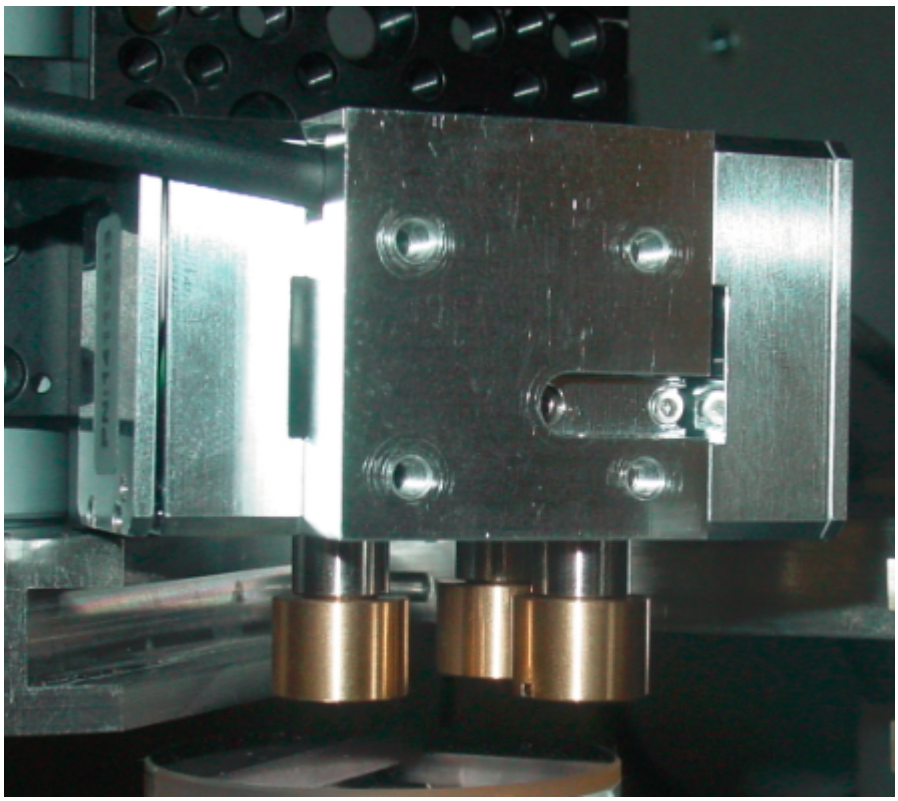

b)

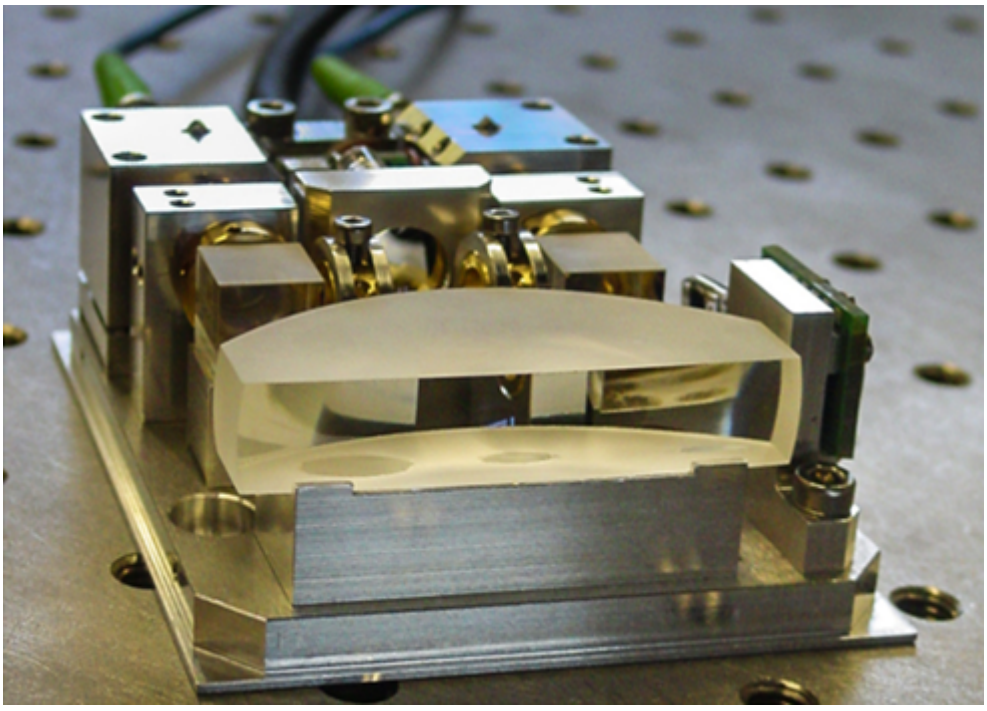

Figure 7 a) Photograph of the combination of three vertical tracking sensors.
b) Photograph of lateral tracking sensor with its cover removed.

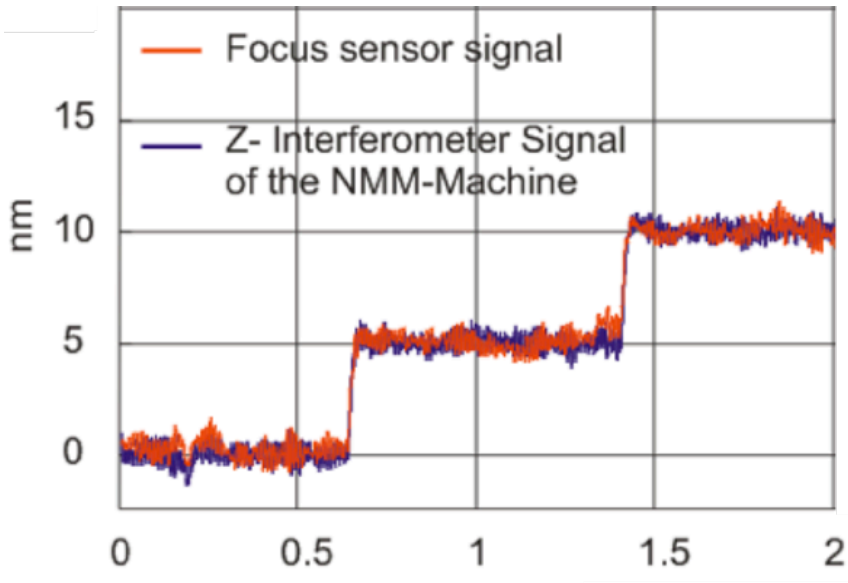

a)

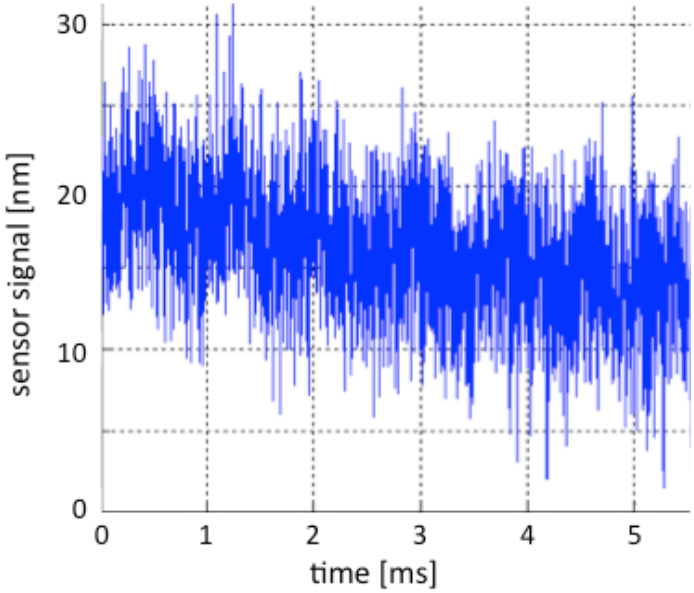

b)

Figure 8: a) Signal of the vertical tracking sensor (red) and signal of the z-interferometer (blue) when changing the distance to the workpiece in 5 nm steps. The abscissa gives the number of measurement points in multiples of 10^4. b) Lateral tracking sensor signal as function of time. The drift is due to athermal instability of the set-up.

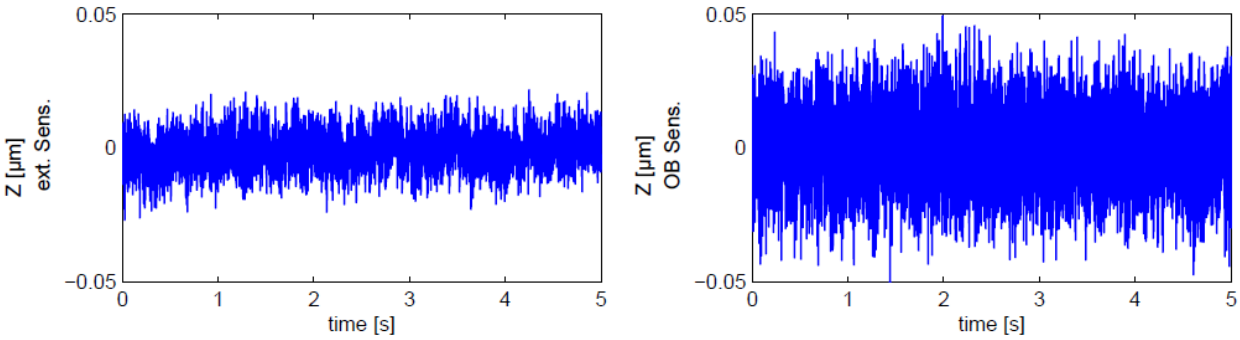

Figure 9 Residual tracking errors when keeping the MP at a constant distance. (Left) Z-Position measured with external sensor. (Right) Z-Position controlled with on-board sensors. The peak-to-valley noise is larger due to the larger sensor noise, however, the real physical movement (see left panel) of the MP is smaller as the system acts as filter for the sensor noise. The noise performance of the vertical on-board tracking sensors still can be improved.

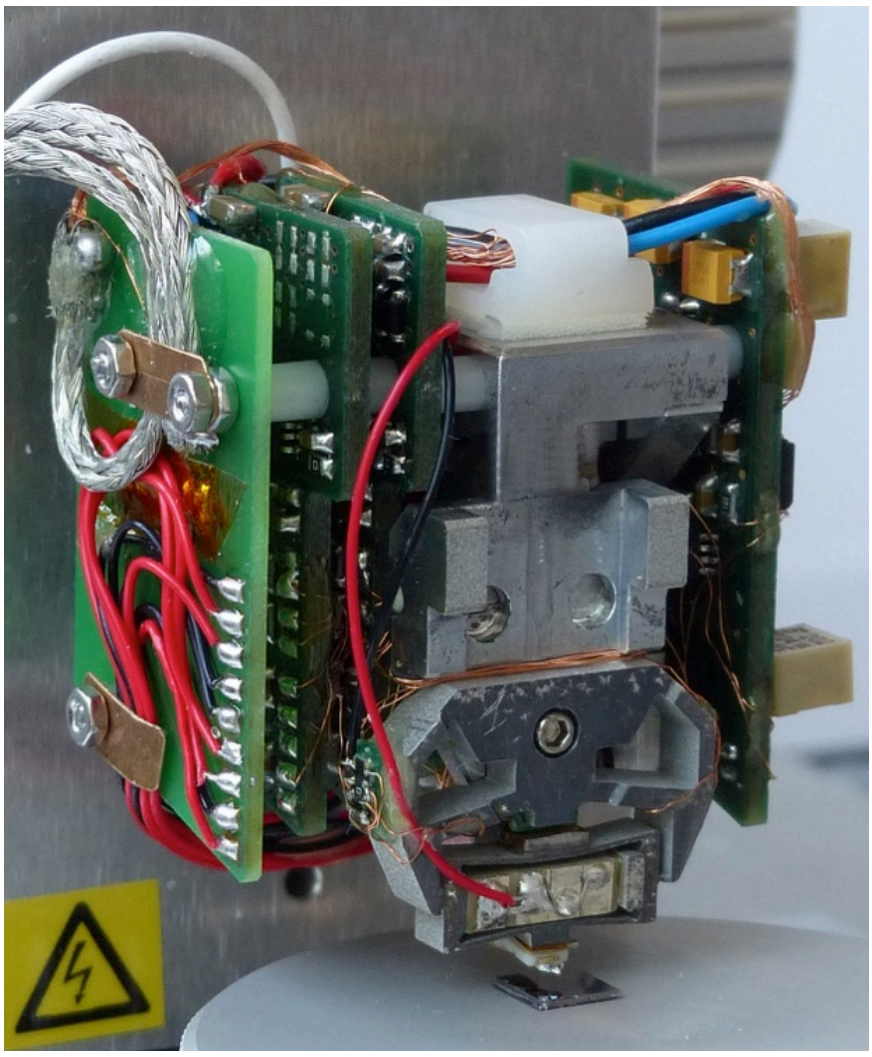

Figure 10: Assembled AFM measurement-head with preamplifiers for position sensors and cantilever deflection sensor (without housing).

a)

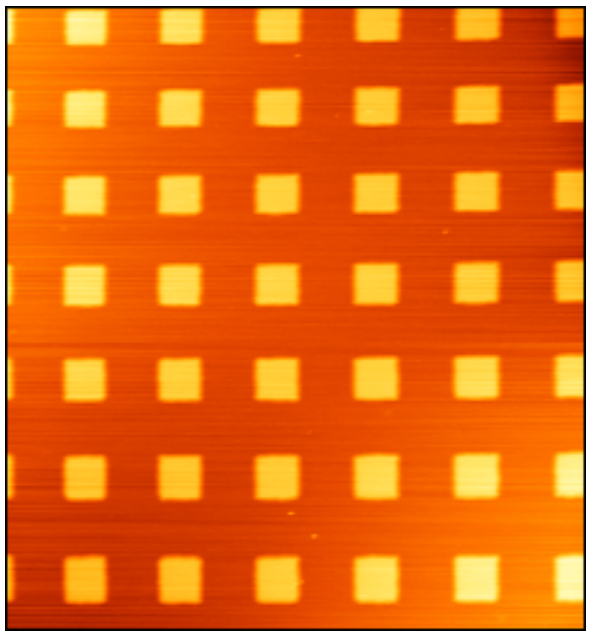

b)

Figure 11: a) Closed-loop AFM image of a 10x10µm pitch calibration grating with 119nm high mesas. Line speed is 600ms. b) Closed-loop AFM image of a 3µm-pitch calibration grating with 22nm step height. Line speed is 50ms. The image size is 20x20µm. Both images recorded in a standard AFM support and optimal laboratory conditions (i.e. not on the MP).

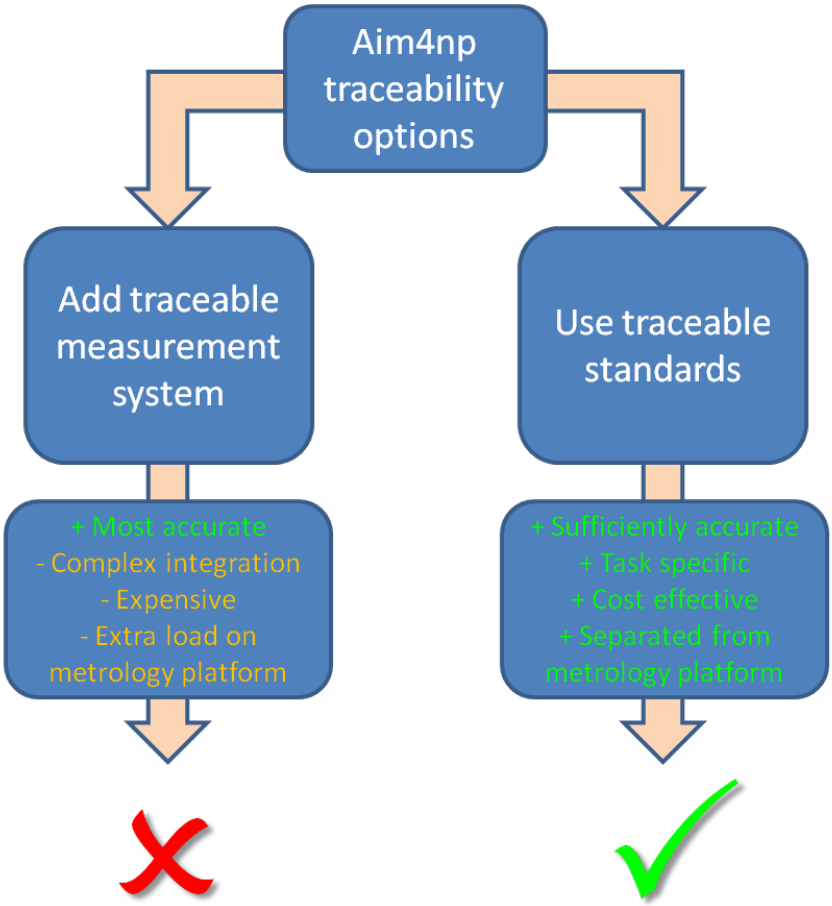

Figure 12 The overall traceability strategy based on traceable standards was considered as the best option for the aim4np project

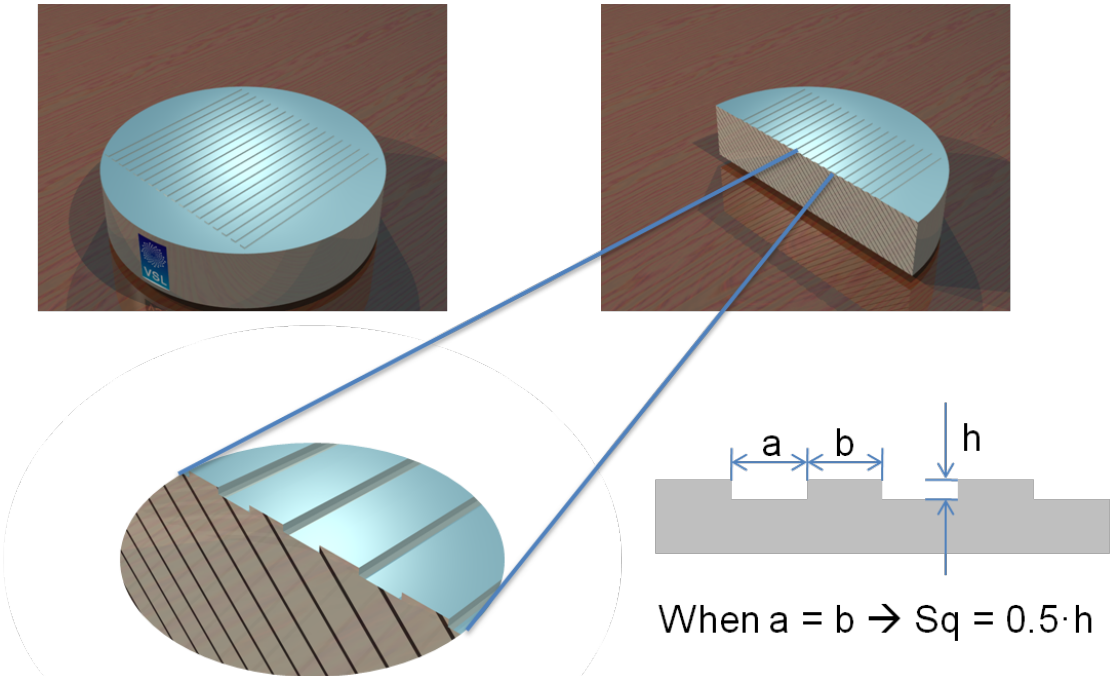

Figure 13 The concept of a practical Sq standard. The geometry provides a simple relation between profile parameters and the resulting Sq value

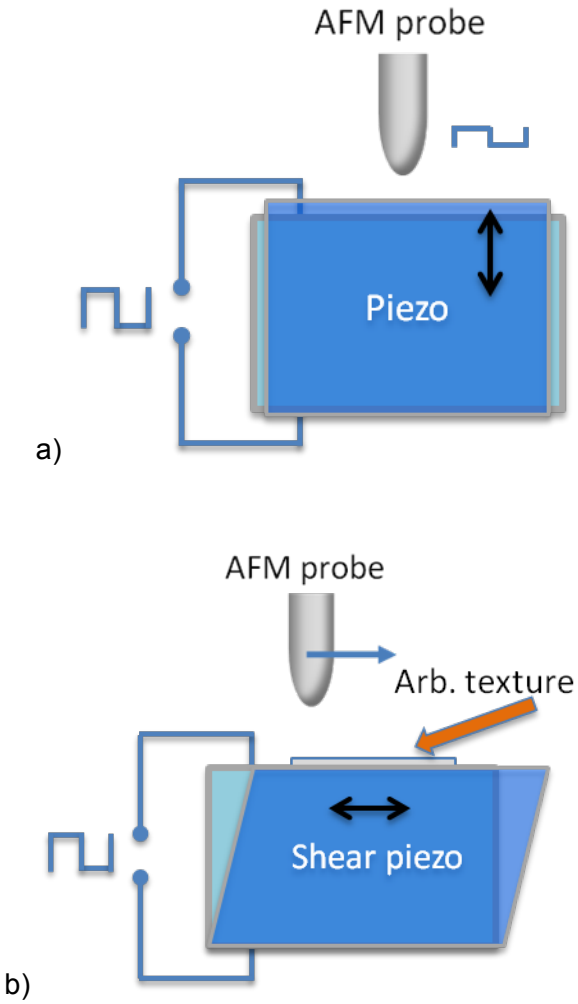

Figure 14 The virtual calibration standards for the height axis of the AFM and for the lateral axes are realized respectively by a longitudinal piezo (a) and a transversal piezo (b).
Both are driven by a waveform generator to provide a tuneable translation.

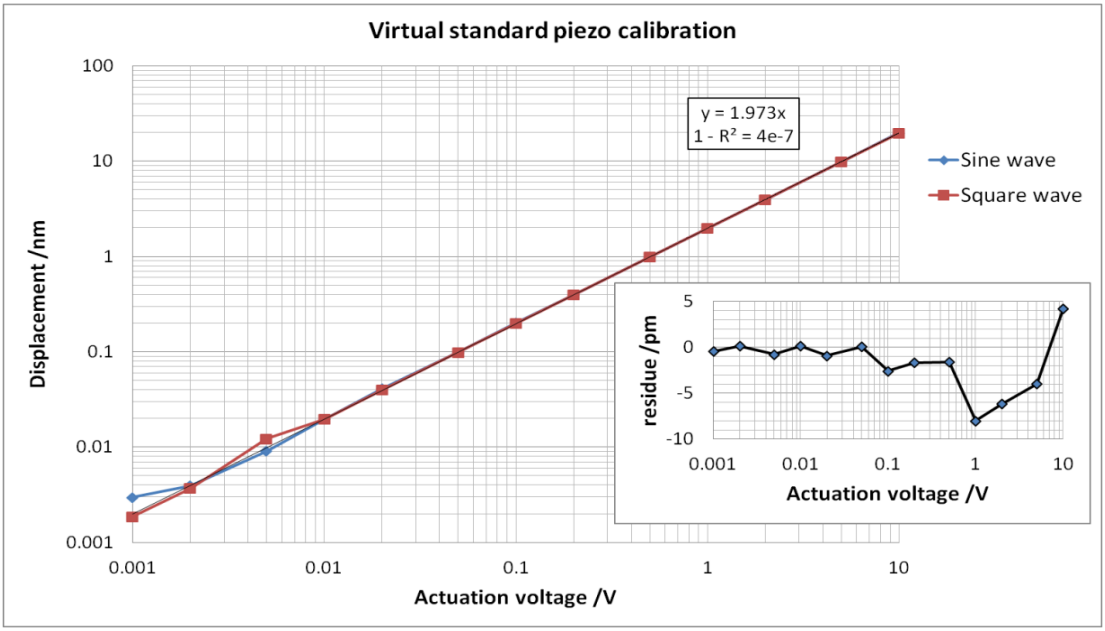

Figure 15 The calibration result to determine the sensitivity of the virtual standard piezo yields a value of 1.973 nm/V. The residue compared to the fit result is shown in the insert.

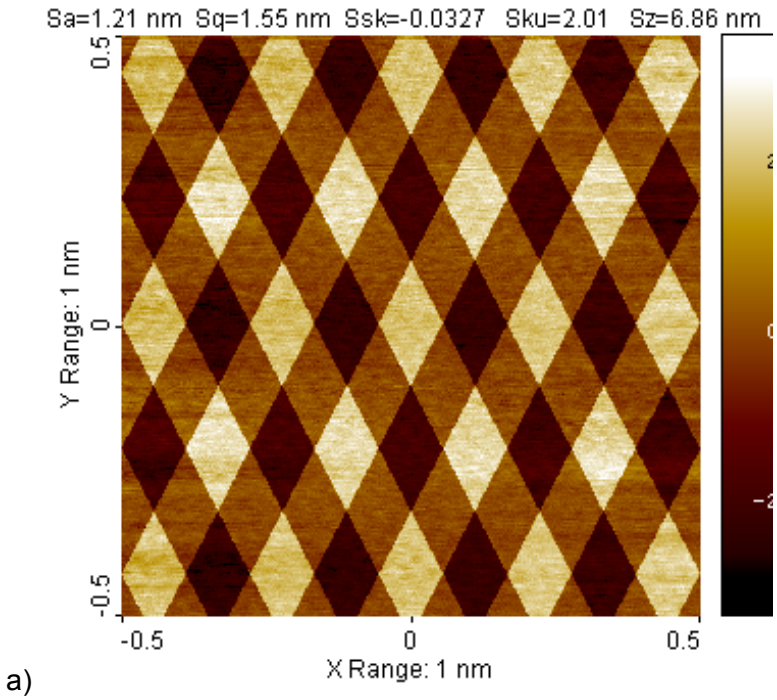

a)

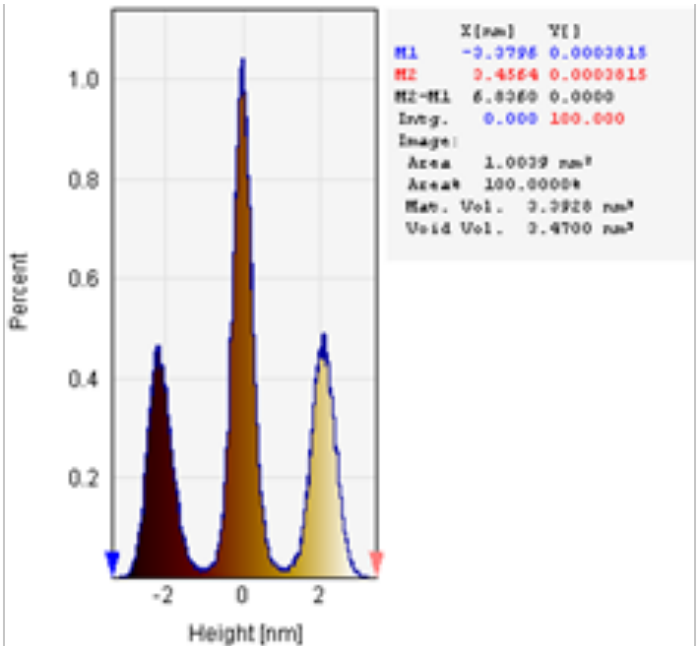

b)

Figure 16 Measurement result on the virtual Sq standard as performed by VSL. The image in (a) shows the difference of the trace and retrace AFM image to eliminate most of the measurement noise. The histogram analysis (b) provides an Sq value of 1.1 nm.

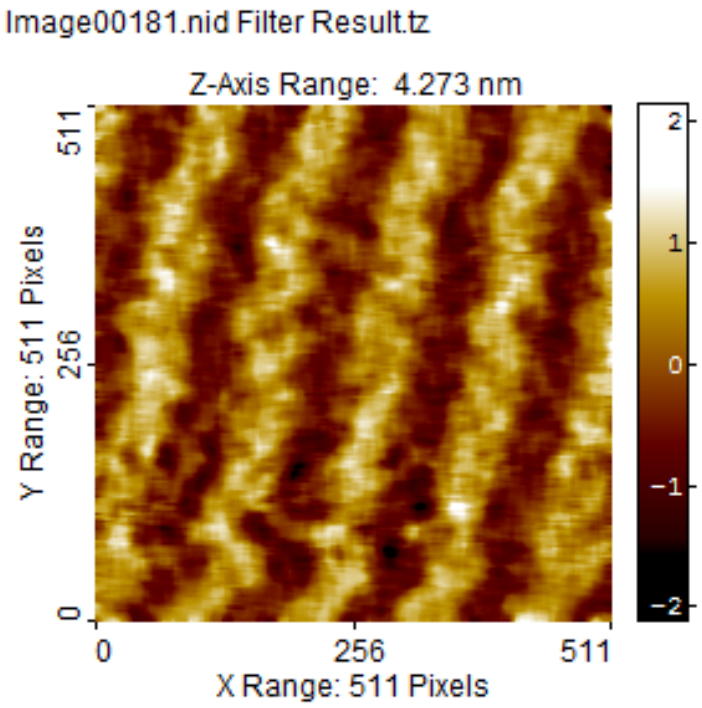

a)

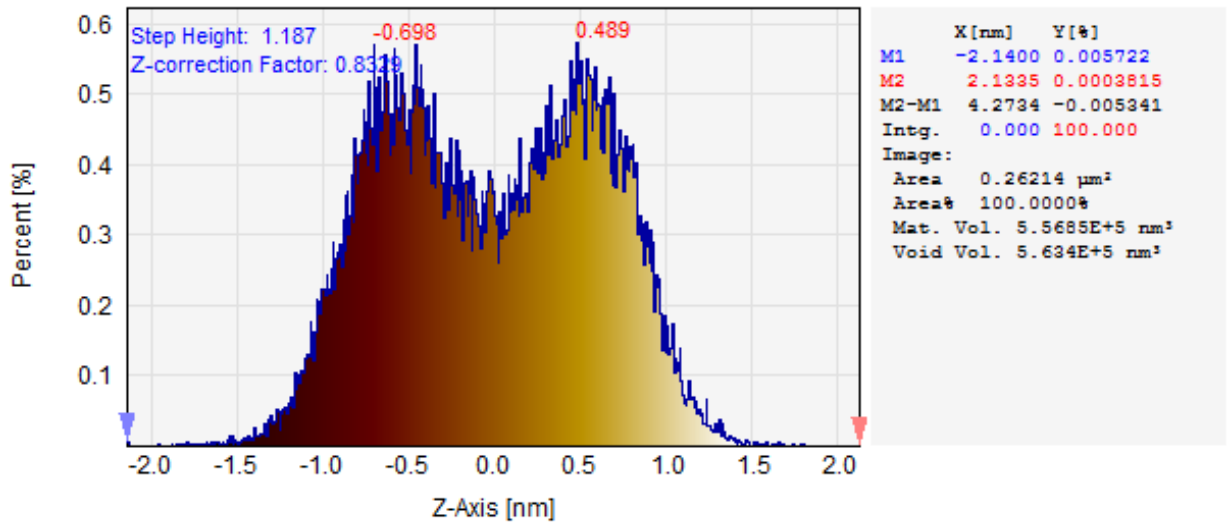

b)

Figure 17 Median filtered measurement for a 1 nm (nominal) step height as measured by the aim4np Nanosurf AFM (a) and histogram analysis (b). The average calibration coefficient calculated from this measurement is 0.83.

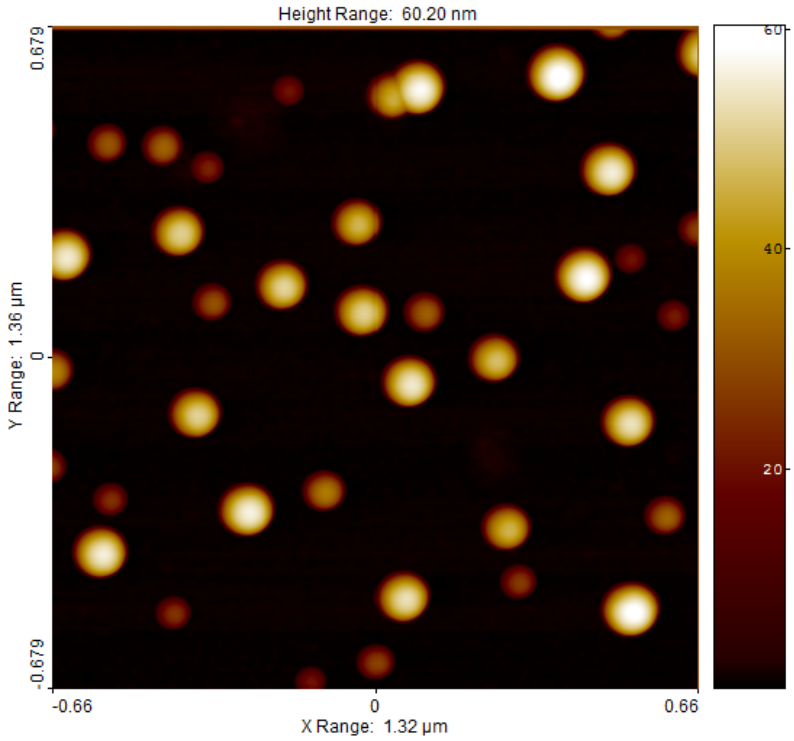

a)

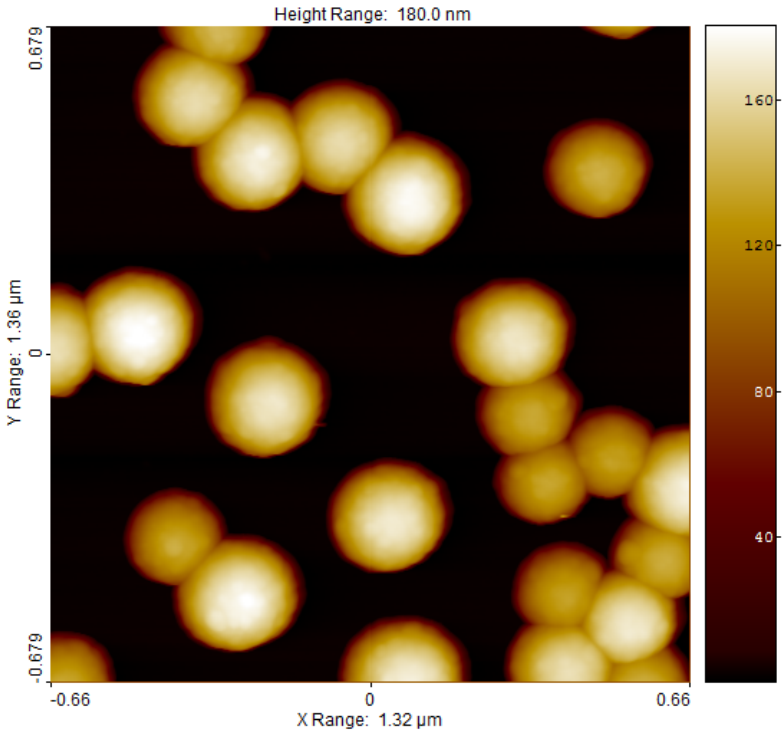

b)

Figure 18 Examples of nanoparticle depositions for the calibration of the AFM probe shape. Polystyrene particles with a wide diameter distribution (a) and silica particles with a bimodal distribution (b) are used to calibrate different parts of the AFM probe. Both images show an area of 1.32µm x 1.36µm in x and y resp.

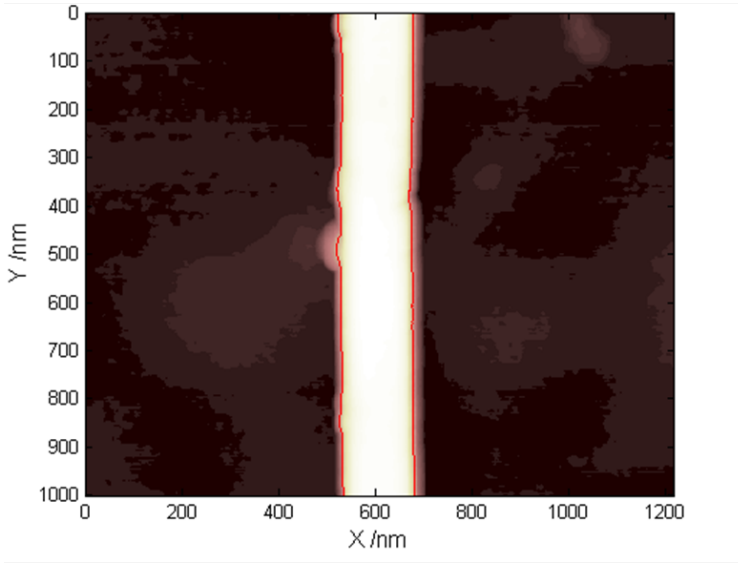

a)

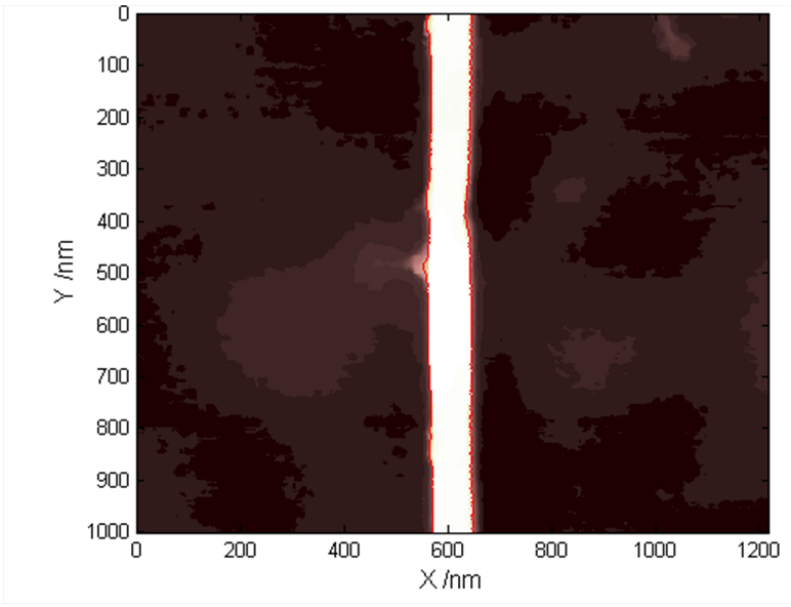

b)

Figure 19 Example of the application of probe shape correction for a measurement of a line structure. The probe had a conical probe with a spherical apex. The line broadening due to the probe shape (left) is reduced to reveal the actual line width (right).

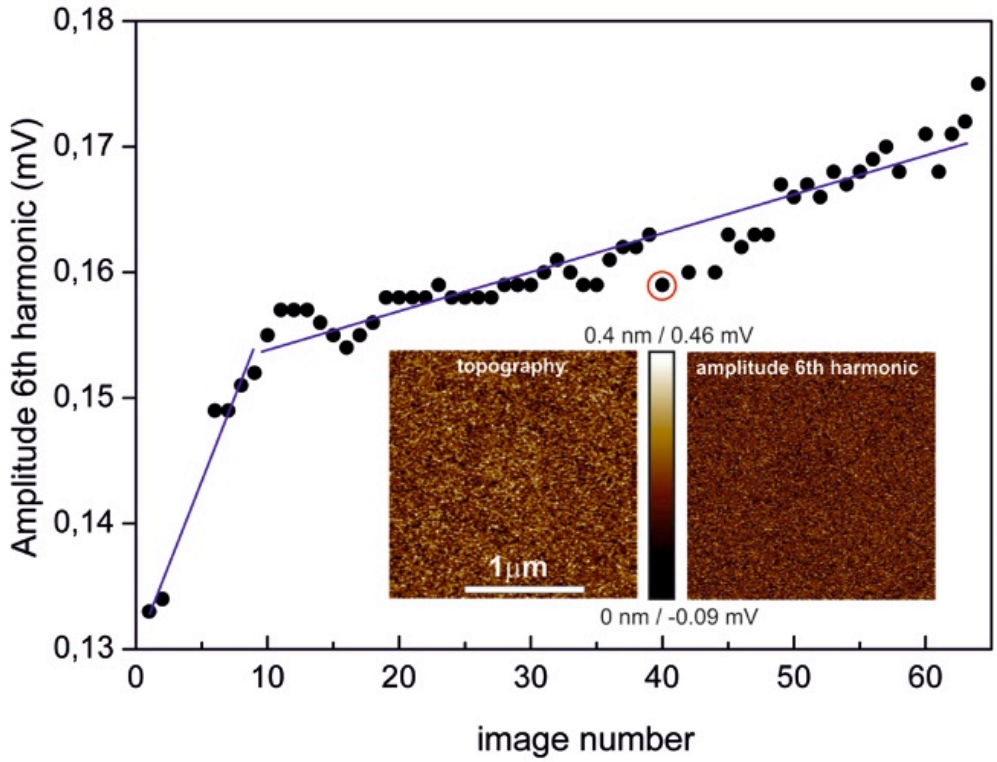

Figure 20: Evolution of the mean value of the amplitude of the 6th harmonic extracted from the amplitude image (right of the inset) simultaneously acquired with the topography (left of the inset) and phase images. Experiments have been performed with a nominally 44 Nm^{-1} rectangular AFM cantilever with resonance frequency f_0 = 350 kHz on silicon surfaces under ambient conditions. The time evolution is expressed in terms of sequentially acquired images. The free oscillation amplitude was set to 30 nm and set-point to 27 nm, respectively. The inset corresponds to the point marked with the red circle. The continuous blue lines are guides to the eye.

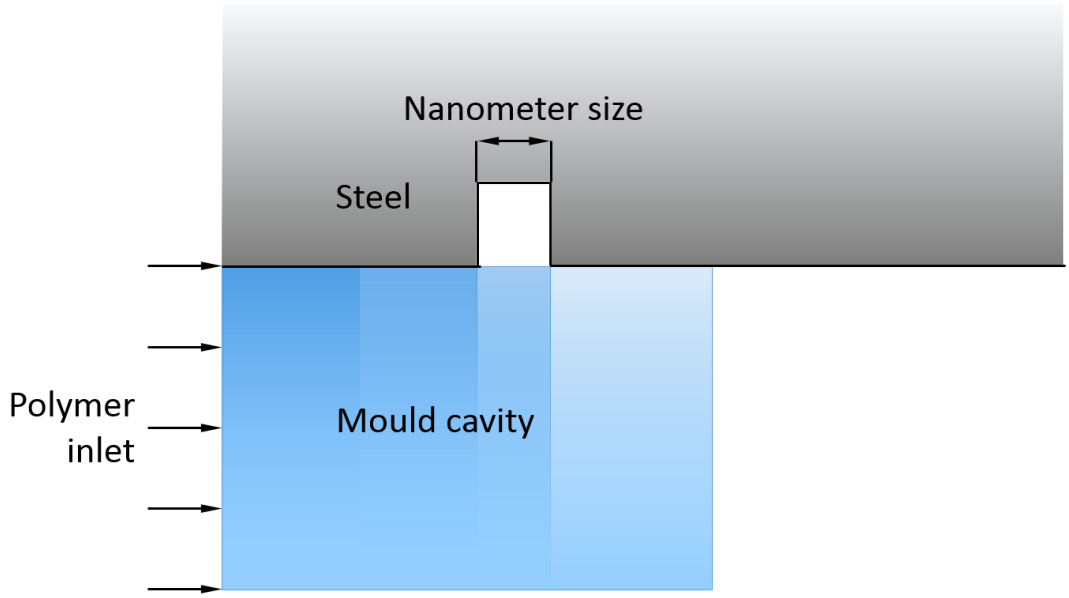

a)

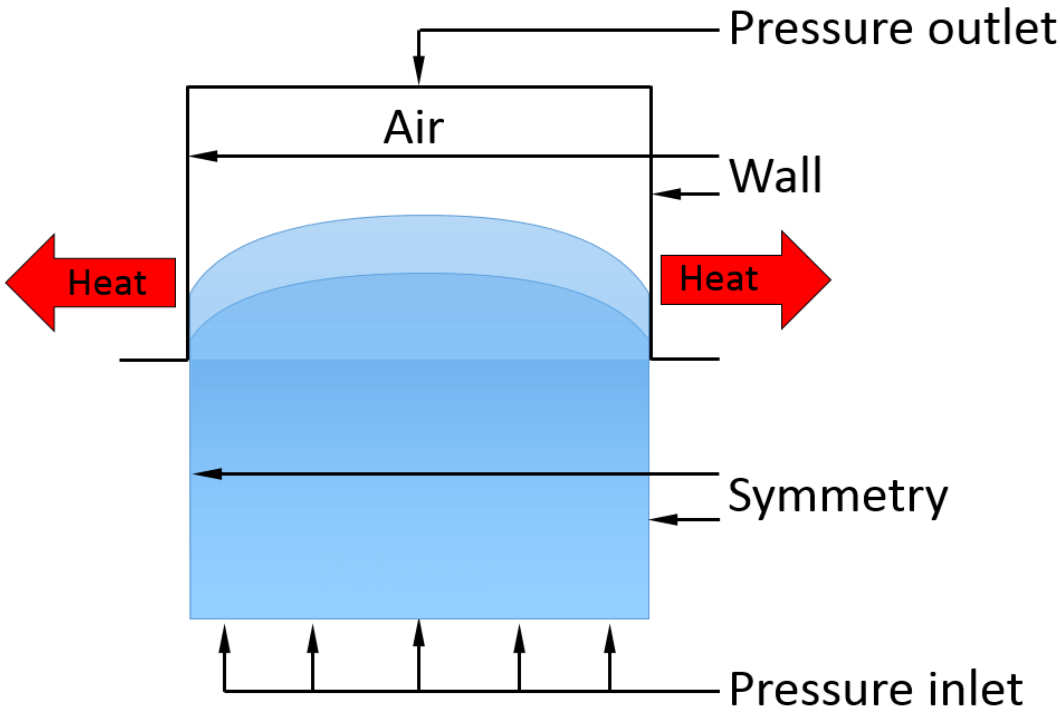

b)

Figure 21: a) Submodelling simulation of the filling of a rectangular cavity with a constant velocity input.
b) Nano simulation of the filling of a 2D cavity. The gradated blue tones indicate the advance of the polymer melt.

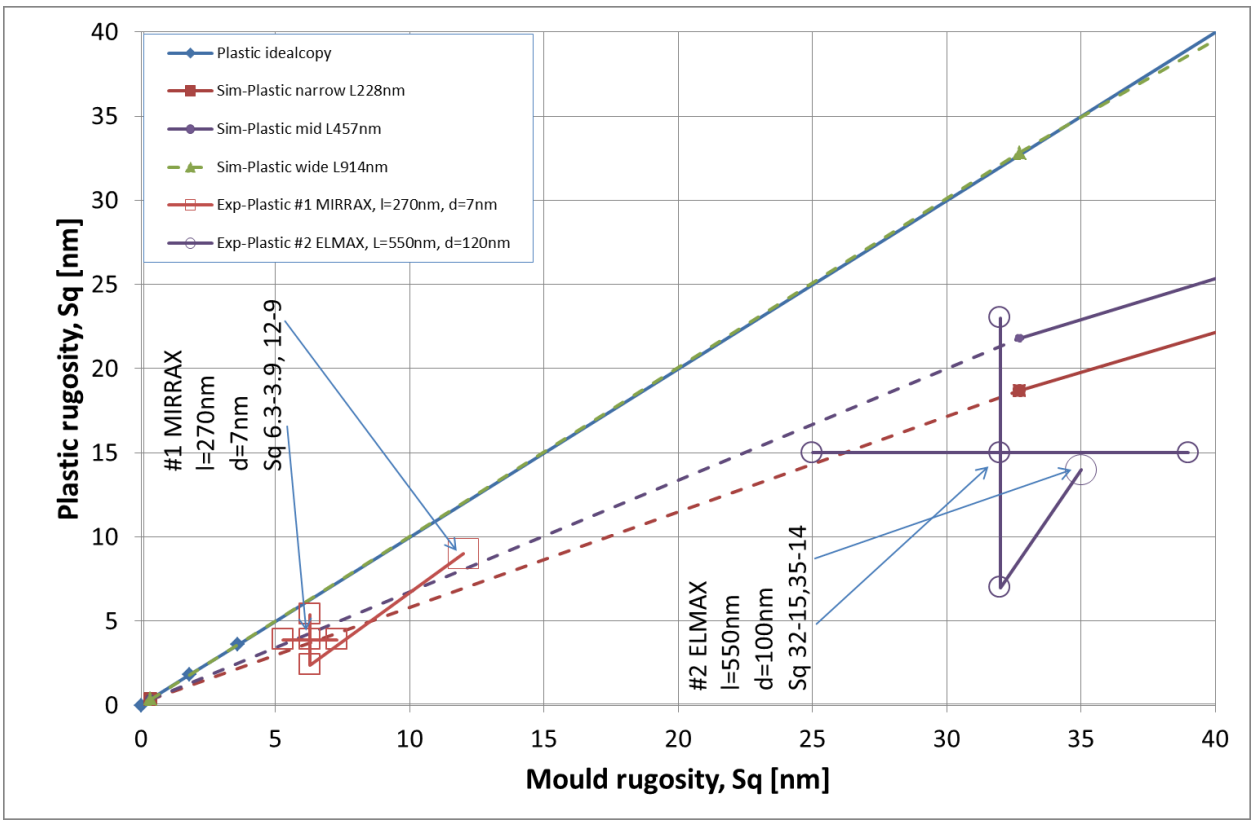

Figure 22: Comparison of surface roughness of the polycarbonate pieces vs. mould roughness. The predicted values (dashed lines) are compared to the experimental points (unfilled squares and circles).

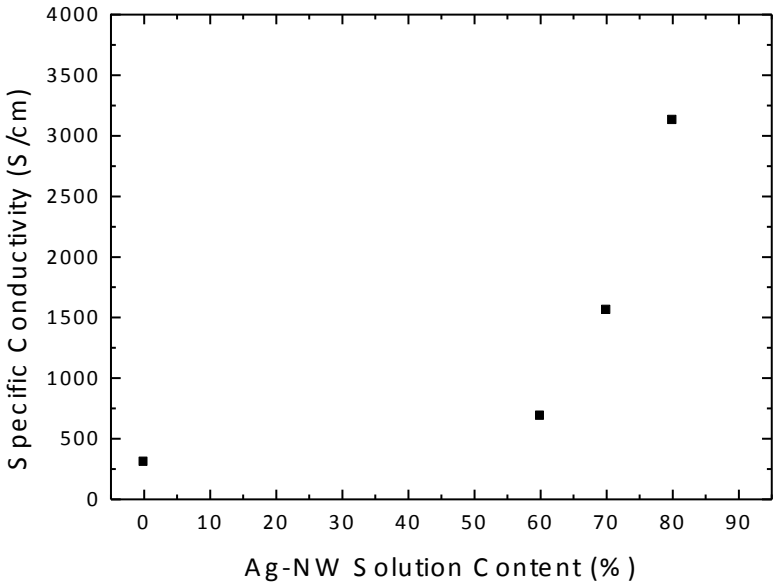

a)

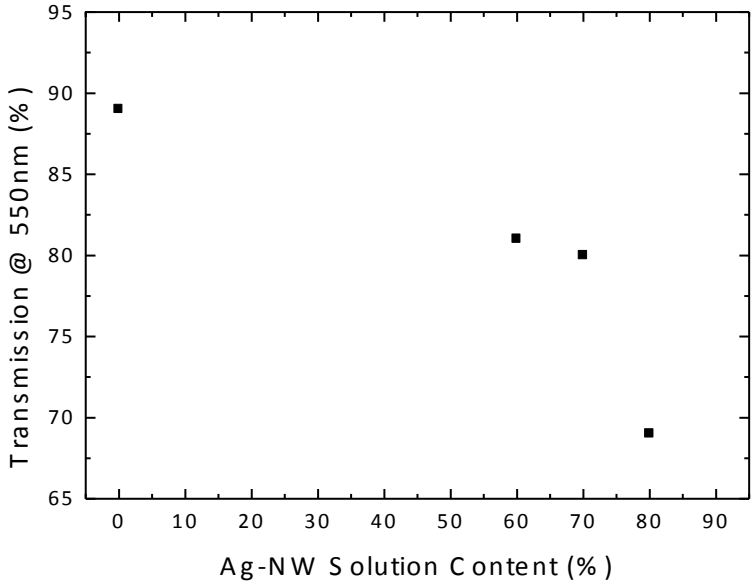

b)

Figure 23 Specific conductivity (a) and optical transmission (b) in dependence on the Ag-NW solution content.

a)

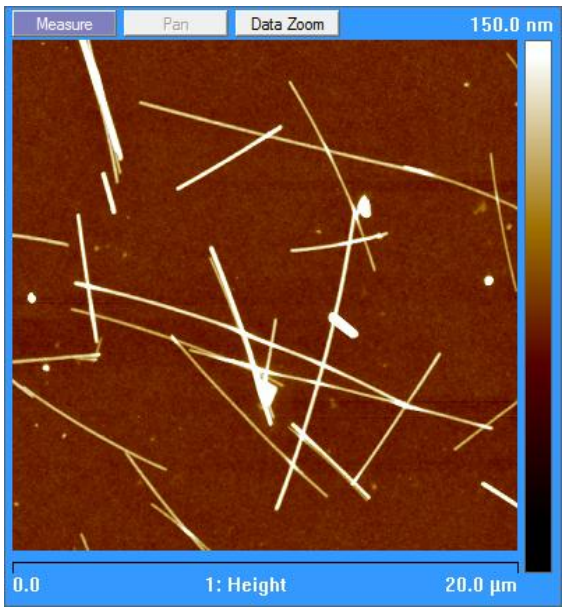

b)

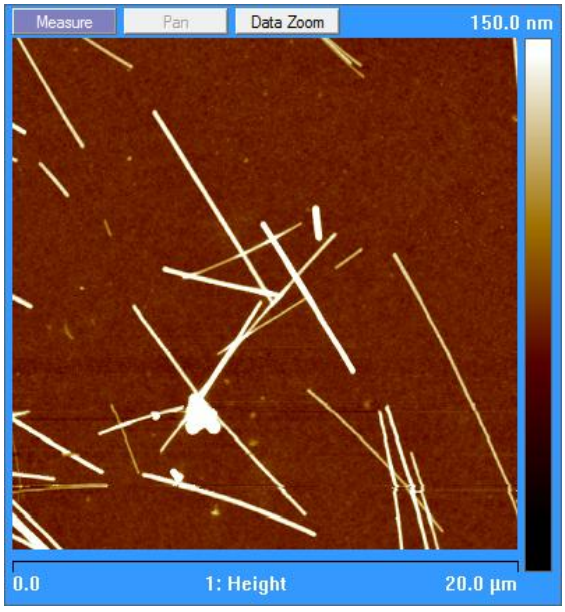

Figure 24 AFM height image of PEDOT:PSS/Ag-NW blend films; Left (a): 60% Ag-NW content, RMS-Roughness Rq=19,1nm; Right (b): 70% Ag-NW content, RMS-Roughness Rq=23,2nm.

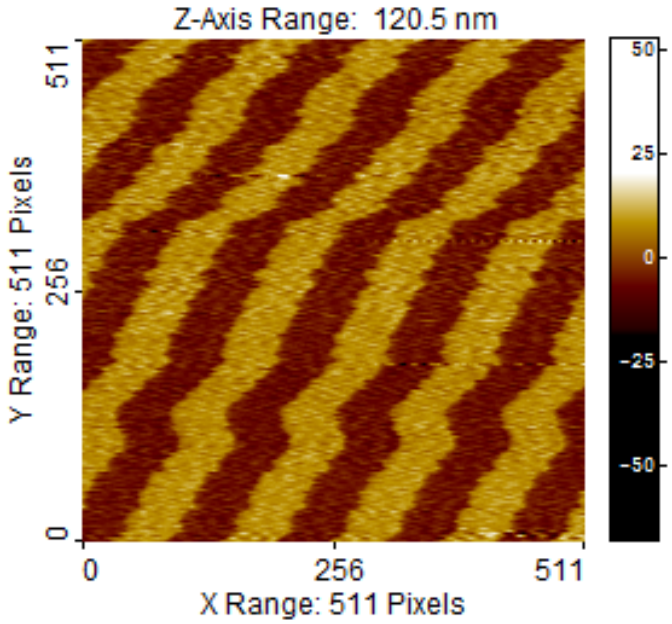

a)

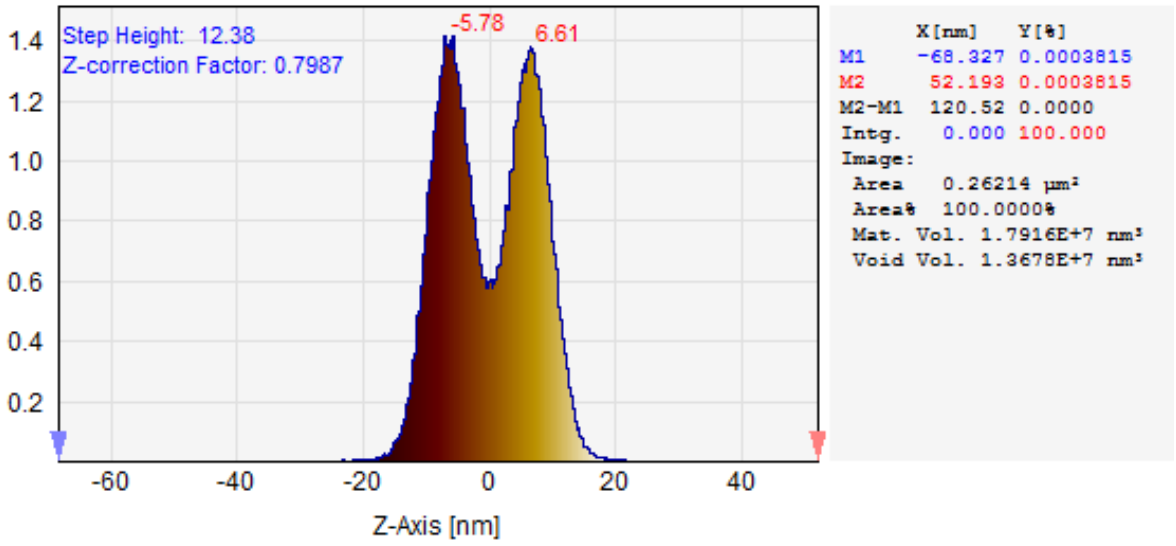

b)

Figure 25 AFM measurement for the 10 nm (nominal) step height actuation. a) AFM data; that non-straight stripes are caused by acquisition characteristics in the AFM electronics. b) Histogram for data analyses. The half-width at half-maximum value (after calibration 3.4nm) indicates the noise caused by the environmental disturbances.

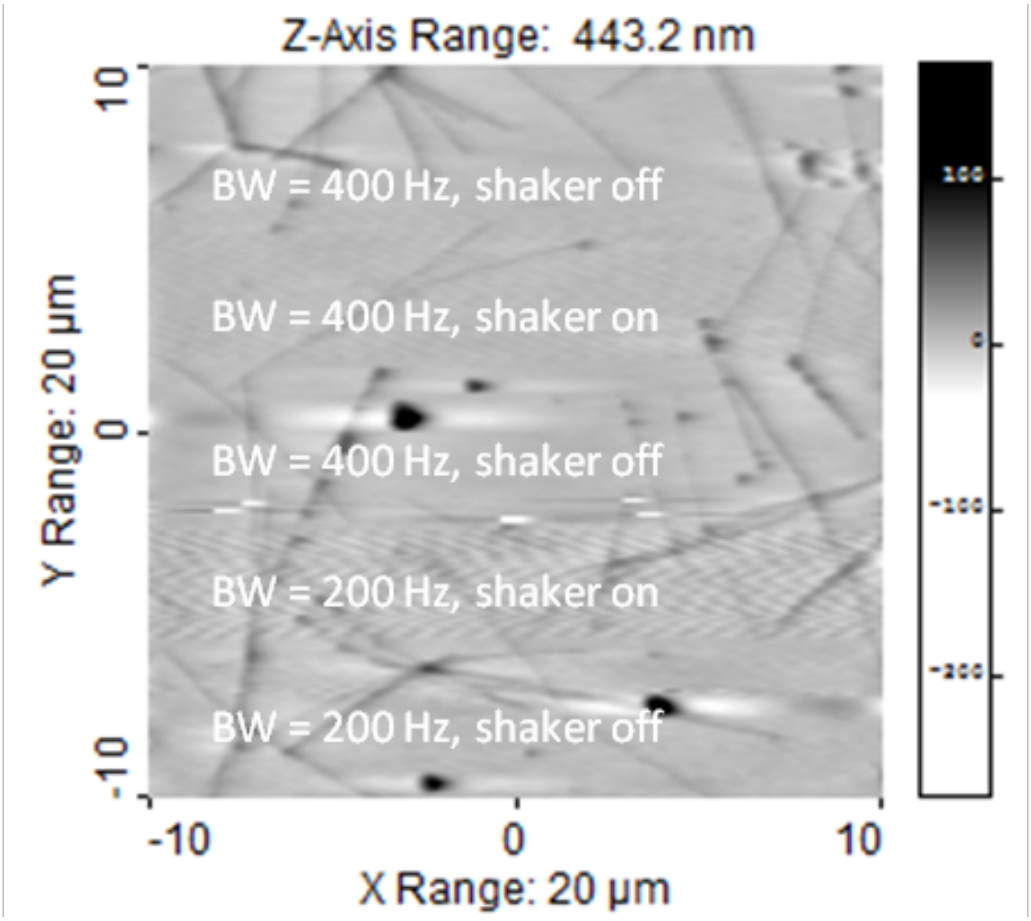

Figure 26 Exp. #10: 5 Vpp; 9.473 kHz;
Scanning frequency: 2 Hz;
Image bottom to top:
Sequence of the experiments:
(Control gain in z direction/Shaker):
[200 Hz / Off]; [200 Hz / On]; [200 Hz / Off];
[400 Hz / Off]; [400 Hz / On]; [400 Hz / Off]

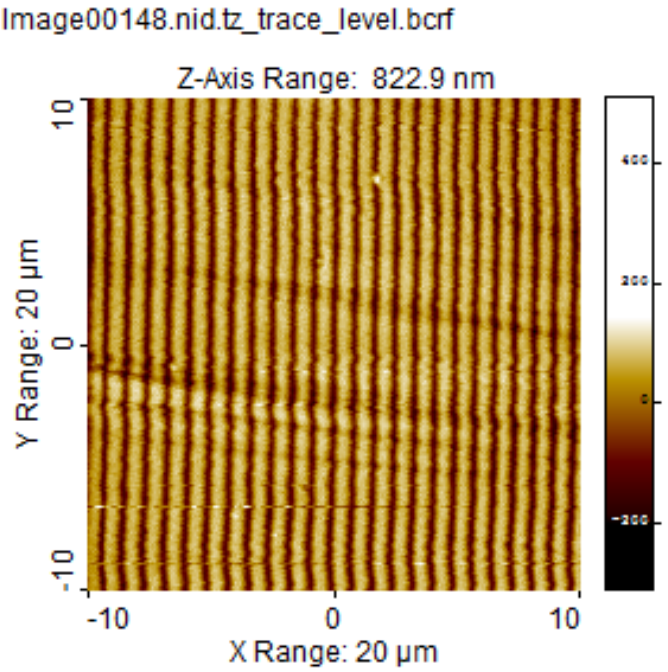
Image00148.nid.tz_trace_level.bcrf
Z-Axis Range: 822.9 nm
Y Range: 20 µm
X Range: 20 µm
10
0
-10
-10
0
10
400
200
0
-200

a)

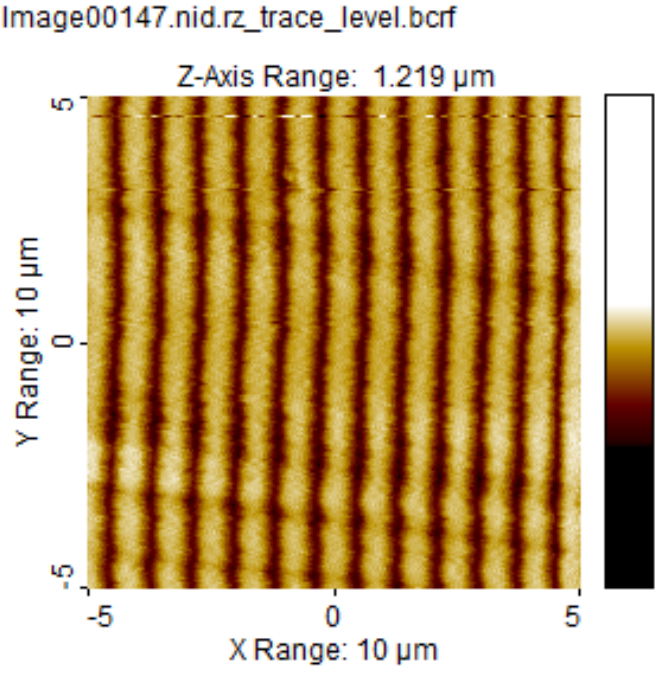
Image00147.nid.rz_trace_level.bcrf
Z-Axis Range: 1.219 µm
Y Range: 10 µm
X Range: 10 µm
5
0
-5
-5
0
5

b)

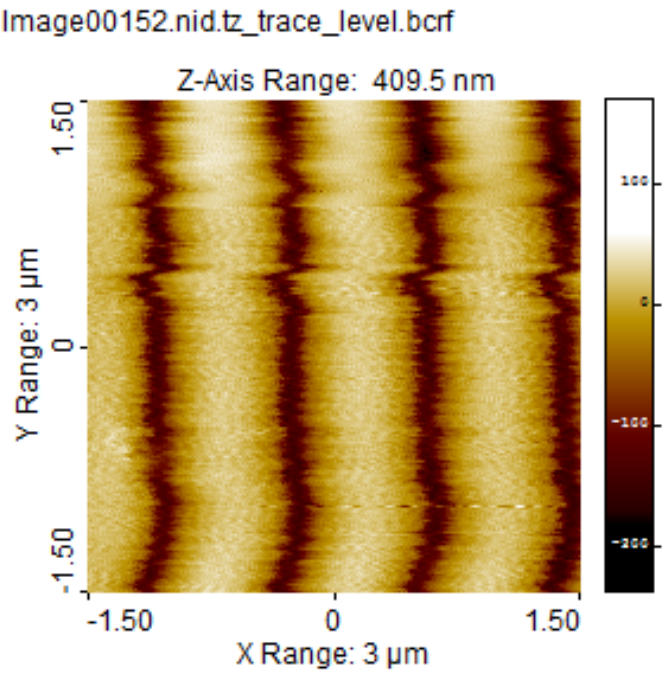

c)

Figure 27 AFM images (20µmx20µm; 10µmx10µm; and 3µmx3µm for resp. a; b;c) of the plastic injection sample (Pitch 0.9 µm; Line separation: 0.3 µm; Line width: 0.5 µm). Defects running under an angle of about 8 degree can be detected.

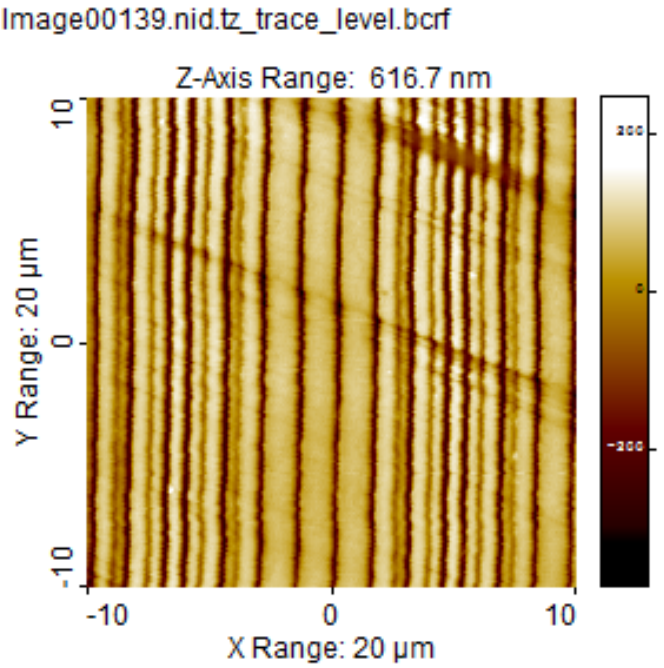
Image00139.nid.tz_trace_level.bcrf
Z-Axis Range: 616.7 nm
Y Range: 20 µm
X Range: 20 µm
10
0
-10
-10
0
10
200
0
-200

a)

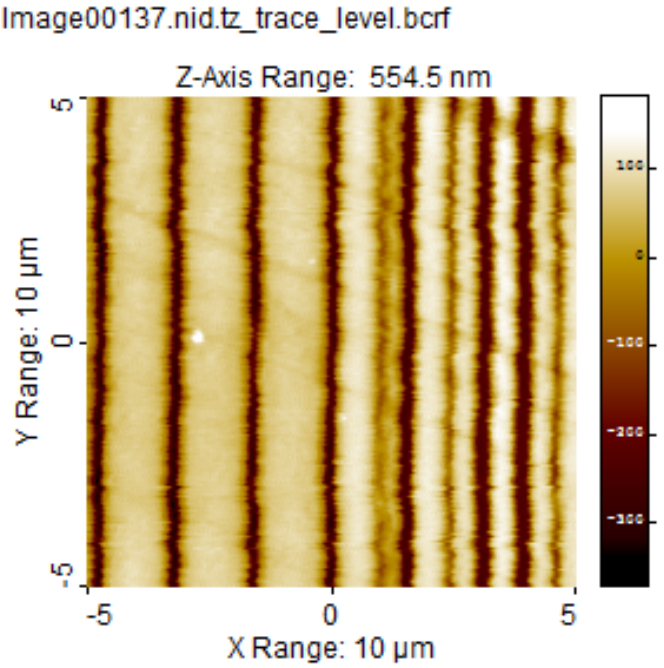
Image00137.nid.tz_trace_level.bcrf
Z-Axis Range: 554.5 nm
Y Range: 10 µm
X Range: 10 µm
5
0
-5
-5
0
5
100
0
-100
-200
-300

b)

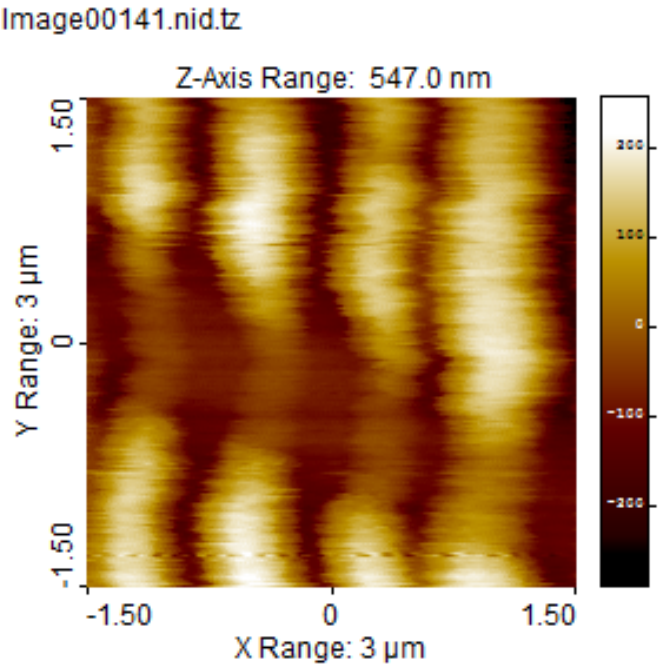

c)

Figure 28 AFM images (20µmx20µm; 10µmx10µm; and 3µmx3µm for resp. a; b;c) of the plastic injection sample, Aperiodic grating. The defects have an angle of about 23 degree relative to the grating.

a)

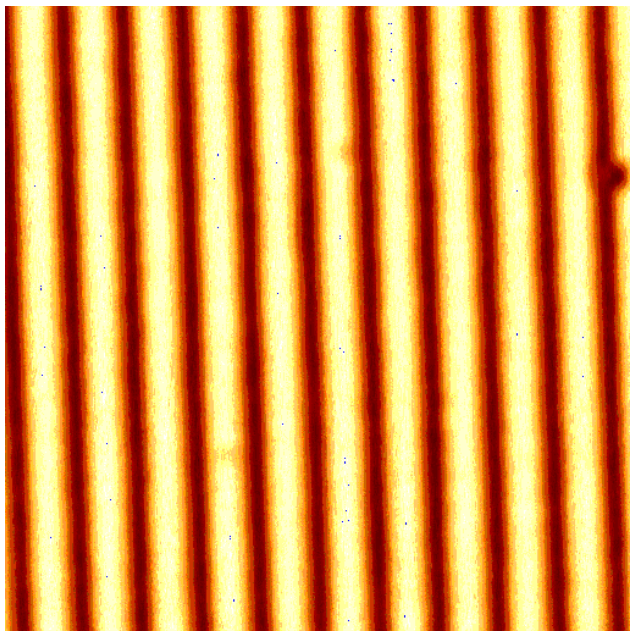

b)

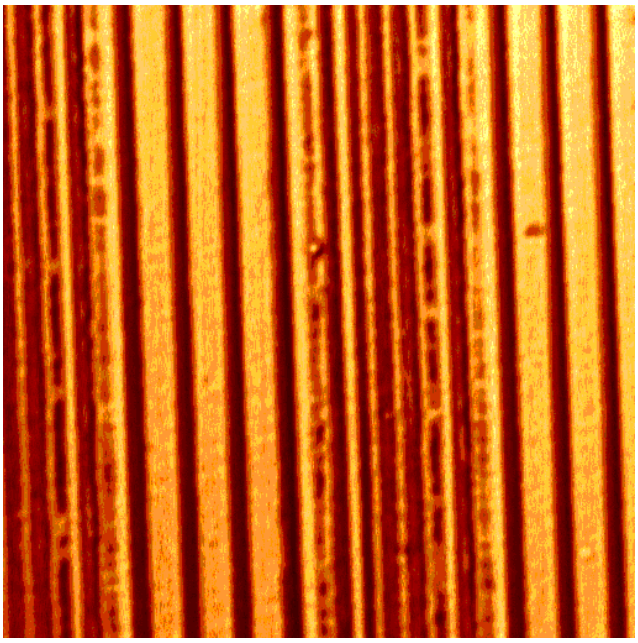

Figure 29 Confocal optical microscope images of sample d5 (a) and e5 (b) respectively.

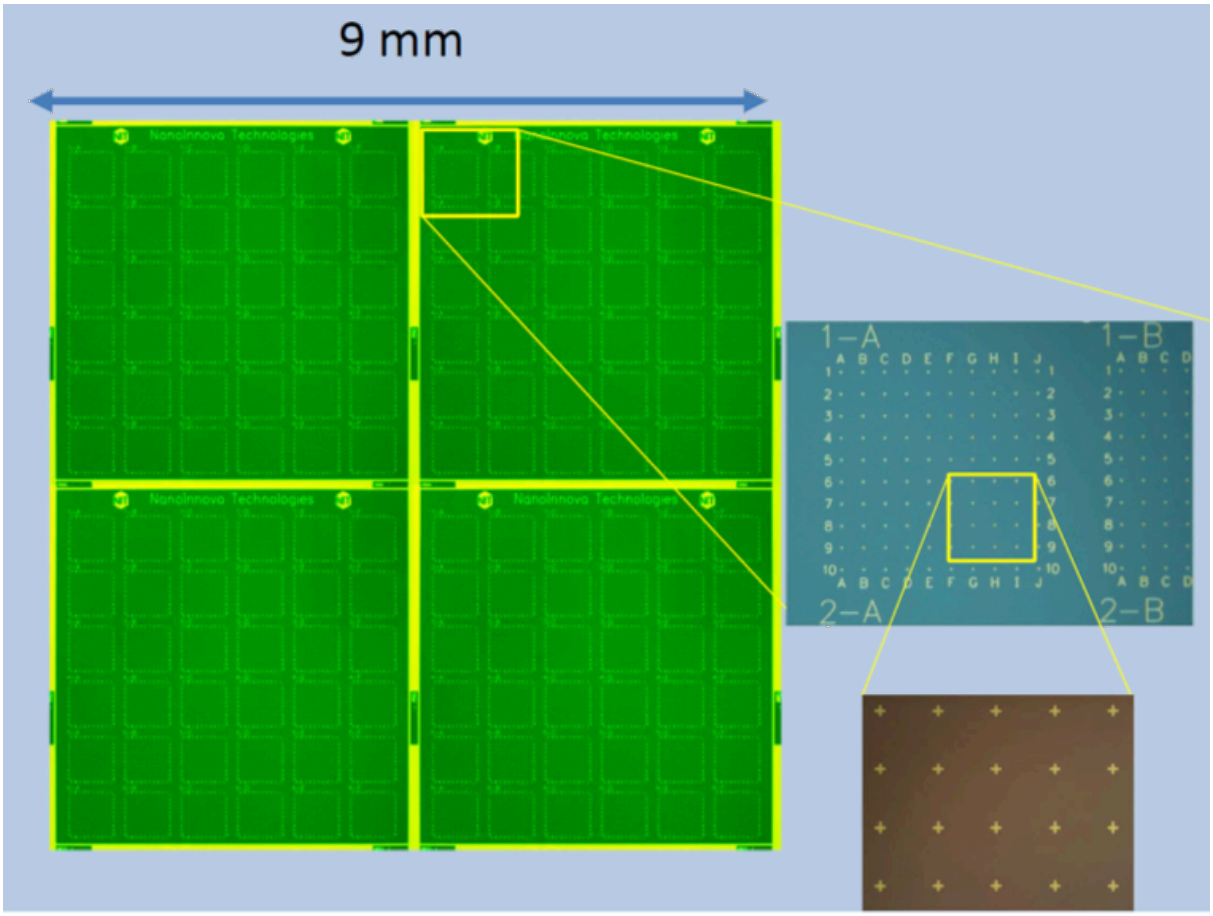

Figure 30 Overview and structure of the navigation sample. The images were recorded with an optical microscope.

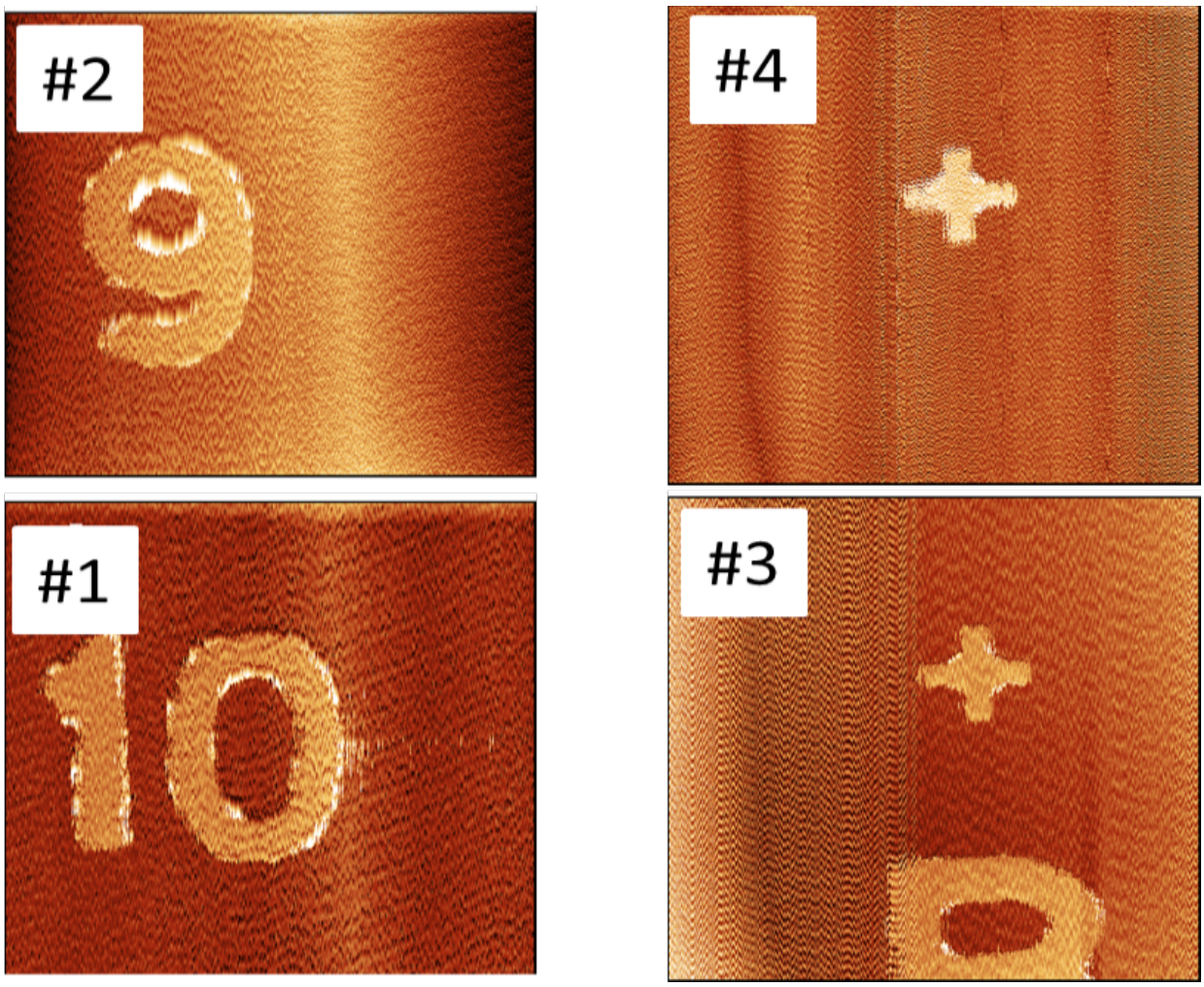

Figure 31 The two AFM images #1 and #2, resp. #3 and #4 were measured after the robot has moved the AFM laterally by 50µm. Between #2 and #3, the tip was exchanged The noise is due to the lateral jittering of the robot, caused by its controller. At least a 3DOF MP would be needed to fully eliminate them.

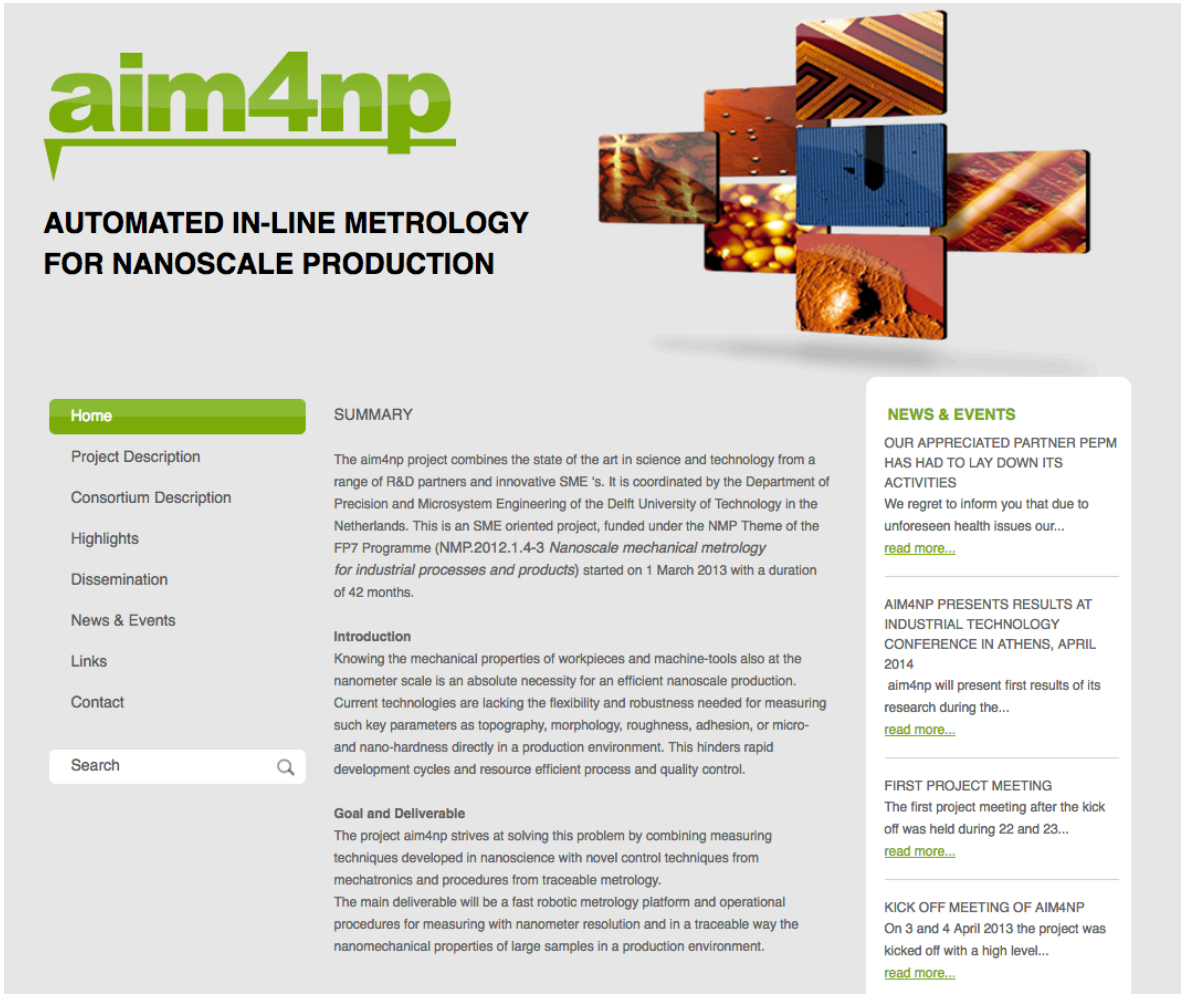

Figure 32 Screen-dump of the start-page of the website www.aim4np.eu